processes

MDPI

Article

The Decomposition of Dilute 1-Butene in Tubular Multilayer Dielectric Barrier Discharge Reactor: Performance, By-Products and Reaction Mechanism

Chao Li [1,2], Xiao Zhu [1,2], Shiqiang Wang [1,2], Yafeng Guo [1,2], Yu Du [1,2], Yinxia Guan [1,2] and Shiya Tang [1,2,*]

[1] State Key Laboratory of Safety and Control for Chemicals, Qingdao 266000, China; lichao.qday@sinopec.com (C.L.); guoyf.qday@sinopec.com (Y.G.)
[2] SINOPEC Research Institute of Safety Engineering Co., Ltd., Qingdao 266000, China
* Correspondence: tangsy.qday@sinopec.com

Abstract: Butene is a typical component of exhaust gas in the petrochemical industry, the emission of which into the atmosphere would lead to air pollution. In this study, a tubular multilayer dielectric barrier discharge (TM-DBD) reactor was developed to decompose 1-butene at ambient pressure. The experimental results show that a decomposition efficiency of more than 99% and CO_x selectivity of at least 43% could be obtained at a specific energy density of 100 J/L with an inlet concentration of 1-butene ranging from 100 to 400 ppm. Increasing the volume ratio of O_2/N_2 from 0 to 20% and the specific energy density from 33 to 132 J/L were beneficial for 1-butene destruction and mineralization. Based on organic byproduct analysis, it was inferred that the nitrogenous organic compounds were the main products in N_2 atmosphere, while alcohol, aldehyde, ketone, acid and oxirane were detected in the presence of O_2. In addition, the contents of formaldehyde, acetaldehyde, ethyl alcohol, acetic acid and propionic acid increased with an increase in specific energy density, but the contents of propionaldehyde, ethyl oxirane, butyraldehyde and formic acid decreased. Three main pathways of 1-butene destruction were proposed involving Criegee intermediates and ozonolysis of the olefins, and the following degradation could be the dominant pathways rather than epoxidation. Overall, the developed TM-DBD system paved the way for scaling up the applications of plasma technology for gaseous pollutant decomposition.

Keywords: 1-butene; decomposition; dielectric barrier discharge reactor; O_2 concentration; oxidation mechanism

Citation: Li, C.; Zhu, X.; Wang, S.; Guo, Y.; Du, Y.; Guan, Y.; Tang, S. The Decomposition of Dilute 1-Butene in Tubular Multilayer Dielectric Barrier Discharge Reactor: Performance, By-Products and Reaction Mechanism. *Processes* **2023**, *11*, 1926. https://doi.org/10.3390/pr11071926

Academic Editor: Muftah H. El-Naas

Received: 17 April 2023
Revised: 17 June 2023
Accepted: 20 June 2023
Published: 26 June 2023

1. Introduction

Butenes are important raw materials for synthetizing masses of industrial chemicals (such as 1,3-butadiene [1] and acetic acid [2]) and polymers (such as linear low density polyethylene and atactic polypropylene [3,4]). Meanwhile, butenes are the typical gaseous pollutants in petrochemical waste gas, which are unwanted byproducts in dehydrogenation and unreacted monomers in polyreactions. Although butenes have low toxicity and exert little effect on human health, their emission into the atmosphere should be controlled to avoid secondary pollution mediated by photochemical reactions [5–7]. Therefore, it is imperative to develop appropriate technology to remove butenes before being emitted into the atmosphere.

At present, there are many conventional methods to remove 1-butene, including adsorption, thermal combustion and catalytic oxidation. However, these techniques have some limitations in VOC treatment. For example, the adsorption method suffers from secondary pollution (such as spent adsorbent and collected organics). Thermal combustion has high natural gas consumption and produces extra CO_2. The catalytic oxidation can work well only at a high temperature, and catalyst poisoning is also a major problem [8]. In comparison, non-thermal plasma (NTP) technology has been widely used for odor and

exhaust gas treatment due to its good decomposition capacity and low operating cost [9,10], especially for low concentration VOCs (<1000 ppm) [11–13]. Additionally, NTP technology also has some specific advantages, such as simple operation, quick switch of equipment, and simultaneous treatment of multiple pollutants. There are many ways to generate NTP, such as glow discharge, corona discharge and dielectric barrier discharge (DBD). Among these methods, DBD can prevent the occurrence of arc discharge and avoid the corrosion of metal electrodes by covering the electrodes with barrier layers [14,15]. Therefore, DBD has been recognized as the most commonly industrial NTP. In the discharge space, the molecules of VOCs can be decomposed and oxidized by highly reactive species, e.g., $O(^1D)$, $O(^1S)$, $O(^3P)$, O^+, $O_2{}^+$, O_3, $N_2(A_3\Sigma_u^+)$ and $N_2(B_3\Pi_g)$, which are produced by collisions between energetic electrons and background gas molecules, such as N_2 and O_2 [16–18]. Thus far, only a handful of studies have been concerned with alkene decomposition by NTP, and most of them focus on the removal of ethylene. Mok et al. [19] reported that alkene and substituted alkene have much higher decomposition rate constants than aromatics and substituted alkane compounds. Aerts et al. [20] studied ethylene decomposition by the global (0D) model and found that atomic oxygen is the dominant destruction species at a low specific energy density (SED) and low inlet concentration, whereas the metastables dominated the destruction process at a high concentration and high SED. In the discharge space, O_2 promotes the mineralization of VOCs but also produces some hazardous organics, e.g., alcohol, aldehyde, ketone, acid, etc. [21–24]. In addition, SED and O_2 concertations also affect the formed CO_x and byproducts [25,26]. The decomposition and mineralization of ethylene can be improved with plasma-catalytic reactors developed by Mok et al. [27–29], and some unwanted byproducts, including O_3 and NO_x, were inhibited at a low ethylene concertation. In conclusion, these researchers offered a rich diversity of methodologies to investigate 1-butene decomposition in the plasma system. However, as an important waste gas during industrial processes, 1-butene decomposition by DBD plasma is still unknown. The comprehensive analysis of the 1-butene decomposition mechanism in NTP would be beneficial to promote the application of NTP technology in industrial VOC management.

In this work, a tubular multilayer dielectric barrier discharge (TM-DBD) reactor was developed for the effective decomposition of 1-butene at ambient pressure. The industrial operation parameters, such as inlet 1-butene concentration, SED and $O_2/(N_2+O_2)$ ratio on 1-butene decomposition, were studied in a DBD reactor. The distribution of organic byproducts was detected by GC-MS analysis under different SED and N_2/air conditions. The decomposition mechanism of 1-butene was proposed in terms of byproduct analysis results.

2. Experimental Setup and Method

2.1. Experimental Setup

As shown in Figure 1, the experimental setup consisted primarily of a gas feeding system, a DBD reactor, a power supply, and electric and gaseous analytical systems. All continuous flow gases were supplied by gas cylinders and were adjusted by mass flow controllers (MFC). The 1-butene was mixed and diluted with N_2 and O_2 in a flask and then fed into the DBD reactor. The gas flow rate was selected at 40 L/min, 60 L/min and 80 L/min, and the initial 1-butene concentration was set at 100 ppm, 200 ppm and 400 ppm, respectively. The O_2 concentration in the fixed flow rate was adjusted by changing the proportions of O_2 and N_2. A tubular multilayer dielectric barrier discharge (TM-DBD) reactor was designed based on a study by Zhang et al. [30]. The TM-DBD reactor was energized by a high-frequency and high-voltage AC power supply (CTP-2000K, China) with sine wave output, which could supply voltage varying from 0 to 30 kV and frequency varying from 1 to 100 kHz. The applied voltage and current were monitored with a digital oscilloscope (Tektronix DPO3054, Beaverton, OR, USA), a high voltage probe (Tektronix P6015A) with an attenuation ratio of 1000:1, and a passive probe (Tektronix TPP0500). Gas samples were collected at the outlet of the DBD reactor. The 1-butene concentration was measured on a gas chromatograph (Agilent 8890B, Santa Clara, CA, USA) equipped with

a flame ionization detector (FID). Organic intermediates were qualitatively analyzed on gas chromatography mass spectrometry (GC-MS) (Agilent 7890B-5973N, America). The concentrations of CO and CO_2 were quantified using a Fourier transform infrared (FTIR) spectrometer (Thermo Fisher, Antaris IGS, Waltham, MA, USA) fitted with a 20 cm long gas cell. The O_3 concentration was monitored by a O_3 analyzer (uSafe 3000, Shenzhen, China). The NO_2 concentration was determined online using a flue gas analyzer (Testo 350, Titisee-Neustadt, Germany).

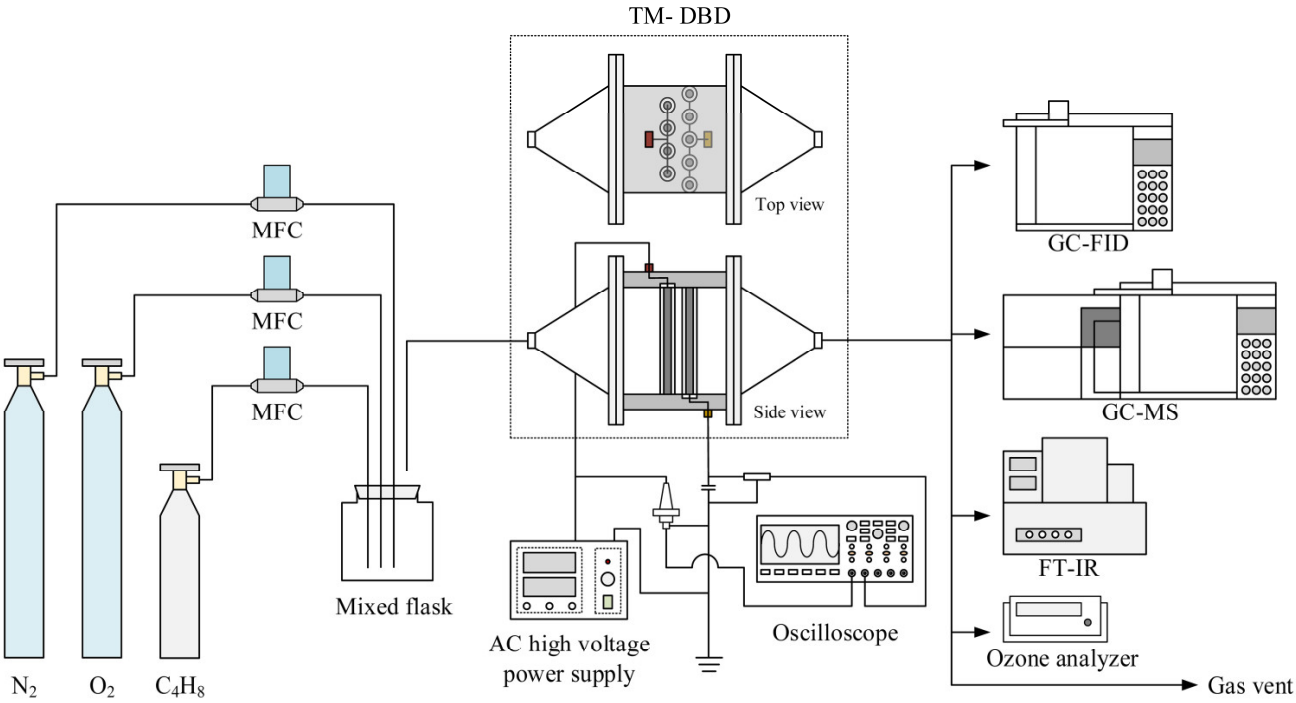

Figure 1. Schematic of the experimental system for 1-butene decomposition in a DBD reactor.

2.2. DBD Reactor

The TM-DBD reactor is shown in Figure 2a and the pinouts were led out from the endpoints of iron powder for connecting high voltage power supply or ground. Each hollow quartz dielectric tube had a wall thickness of 1.5 mm, outer diameter of 10 mm and length of 80 mm. All electrodes were divided into 2 layers arranged in parallel. Adjacent electrodes were placed in every layer evenly with a gap distance of 4 mm. One layer consisting of 4 electrodes was connected with a high voltage power supply, acting as the discharge electrodes. The other layer, consisting of 5 electrodes, was connected with the earth, serving as the ground electrodes. The gap distance between the adjacent discharge electrode and the ground electrode was 3.8 mm. The gas could be treated through the "V" shape of the discharge spaces, which were located between the discharge electrodes and two adjacent ground electrodes. The cross section of gas through the reactor had a height of 80 mm and a width of 60 mm. Figure 2c shows the actual discharge conditions of the TM-DBD reactor in this experiment.

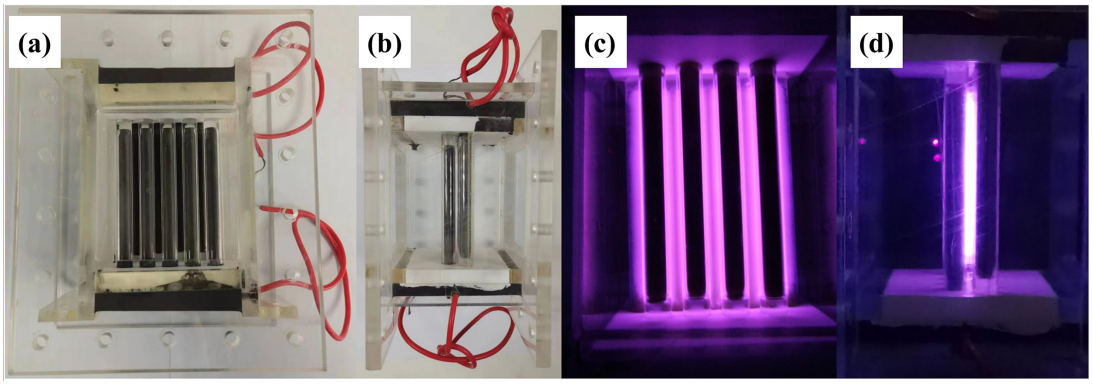

Figure 2. The configuration of the TM-DBD reactor in (**a**) cross-sectional view and (**b**) side view, as well as (**c**) the discharge picture of cross-sectional view and (**d**) the discharge picture of side view.

2.3. Measurement Methods

The energy consumed in the TM-DBD reactor was calculated using the voltage-charge (V-Q) Lissajous method [31]. The specific energy density (SED) was defined as the discharge power (W) divided by the total gas flow rate (L/min), which was calculated using the following relations:

$$\text{SED(J/L)} = \frac{\text{Discharge power}}{\text{Gas flow rate}} \times 60 \quad (1)$$

The percentage of decomposition efficiency (DE) and selectivities toward CO, CO_2 and CO_x were obtained based on the following equations:

$$\text{DE}(\%) = \frac{[C_4H_8]_i - [C_4H_8]_o}{[C_4H_8]_i} \times 100 \quad (2)$$

$$\text{CO selectivity}(\%) = \frac{[CO]_o}{4 \times ([C_4H_8]_i - [C_4H_8]_o)} \times 100 \quad (3)$$

$$CO_2 \text{ selectivity}(\%) = \frac{[CO_2]_o}{4 \times ([C_4H_8]_i - [C_4H_8]_o)} \times 100 \quad (4)$$

$$CO_x \text{ selectivity}(\%) = \text{CO selectivity} + CO_2 \text{ selectivity} \quad (5)$$

where $[C_4H_8]_o$ and $[C_4H_8]_i$ are the concentrations of 1-butene at the inlet and outlet of the TM-DBD reactor, respectively.

3. Results and Discussion

3.1. 1-Butene Decomposition

The capacity of the TM-DBD reactor toward the destruction of 1-butene was evaluated at different initial 1-butene concentrations and specific energy density (SED). In this series of experiments, a fixed $O_2/(N_2+O_2)$ volume ratio of all the carrier gases was set at 20% for simulating air. As shown in Figure 3a, the decomposition efficiency of 1-butene increased with increasing SED at any inlet concentration until complete degradation. Specifically, 1-butene decomposition efficiency increased from 91.2% to nearly 100% with elevating SED from 33 to 66 J/L at an inlet 1-butene concentration of 200 ppm. The SED for attaining complete 1-butene degradation required at least 33 J/L, 66 J/L and 101 J/L when inlet concentrations were 100 ppm, 200 ppm and 400 ppm, respectively. The CO_x selectivity could directly reflect the mineralization extent of 1-butene because CO and CO_2 were the main decomposition products of 1-butene after plasma treatment. Figure 3b shows that CO selectivity was significantly higher than CO_2 selectivity. Notably, it was found that the CO_2 selectivity increased remarkably with the increase of SED, but the increase of CO selectivity was not evident under the same condition. For example, when the inlet 1-butene

concentration was 400 ppm and SED increased from 33 to 203 J/L, the CO_2 selectivity rose rapidly from 4% to 13%; however, the CO selectivity rose slowly from 33% to 35%, which was higher than CO_2 selectivity. These results could be attributed to the fact that CO was much more easily produced than CO_2 in air plasma at atmospheric pressure, and these two oxidation products were generated through different paths (discussed in Section 3.4). Even though both oxidation processes could be enhanced with the increase of SED, CO selectivity increased slightly while an evident increase of CO_2 selectivity was observed. The reason might be that an increase of SED promoted the production of CO; however, most of the generated CO was subsequently consumed to synthesize CO_2 in the presence of extensive active particles.

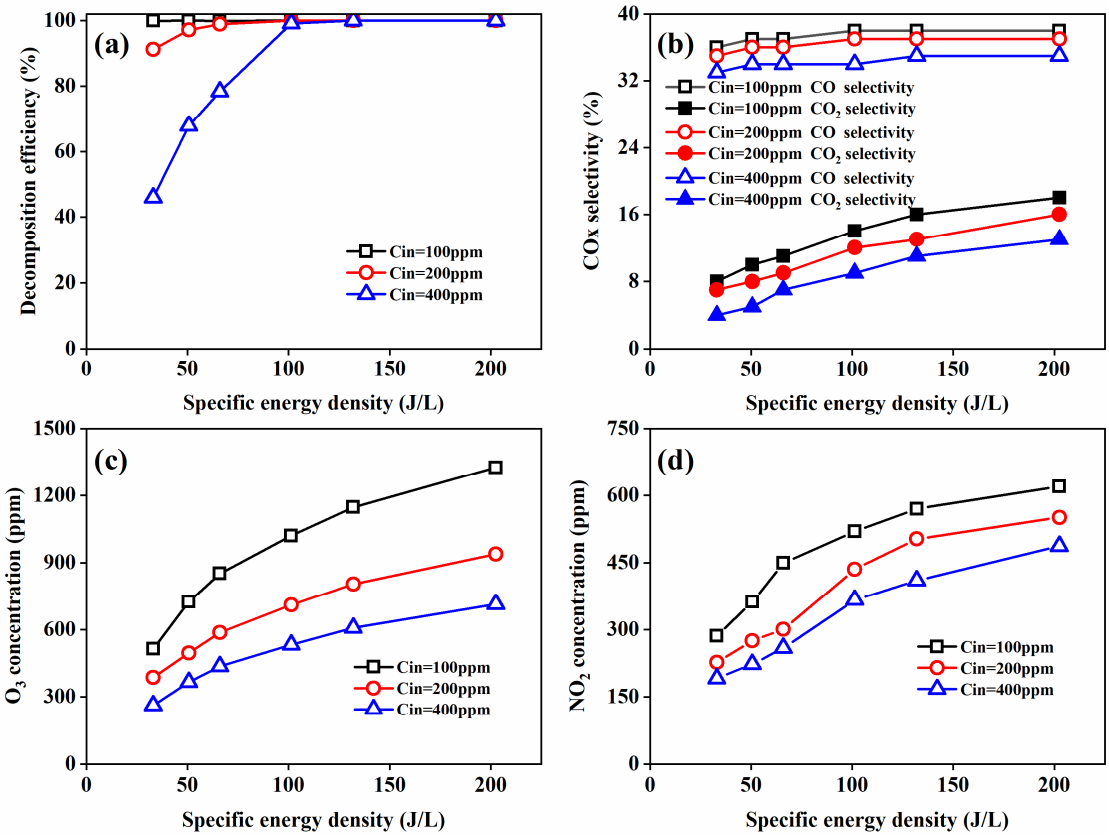

Figure 3. Effect of SED on the decomposition efficiency (**a**), CO/CO_2 selectivity (**b**), as well as the yield of O_3 (**c**) and NO_2 (**d**).

In addition, Figure 3a,b indicates that lower inlet 1-butene concentration gained higher decomposition efficiency (under the state of incomplete degradation) and low CO/CO_2 selectivity. Taking the SED of 51 J/L and inlet 1-butene concentration of 100 ppm as an example, the decomposition efficiency, CO selectivity and CO_2 selectivity were 100%, 37% and 10%, respectively, while the results decreased to 68%, 34% and 5%, respectively, at an inlet 1-butene concentration of 400 ppm. The reason for this phenomenon was more possibilities for less organic molecules to react with highly reactive species in the same discharge space [32].

O_3 and NO_x were the main inorganic byproducts during the plasma treatment process, which should also be measured in the VOC decomposition process. In the air plasma discharge system, these two gaseous compounds were generated via dissociation, excitation and ionization. First, the excited-state atomic nitrogen N(^{2}D) and N(^{2}P), as well as excited-state molecular nitrogen $N_2(A^3\Sigma_u^+)$ were produced by electron collisions with N_2 in Equations (6)–(8) [33,34]. These reactive species reacted with O_2 to generate NO and atomic O, as shown in Equations (9)–(11). In addition, the electron collisions with O_2 also produced the atomic O in Equation (12). O_3 was generated from atomic O via

reactions with O_2 and M in Equation (13), where M could be either O_2 or N_2 [35,36]. NO_2 was detected as a major NO_x species, but no NO was detected in the gas treated by plasma because of the oxidization of O_3 and atomic O, as shown in Equations (14) and (15) [37]. As the equations shown, O_3 and NO_x are both involved in the generation and consumption of "useful" active species, such as atomic O and O_2, which could directly oxidize VOC compounds.

$$e + N_2 \rightarrow e + N\left(^2D\right) + N\left(^2D\right) \quad (6)$$

$$e + N_2 \rightarrow e + N\left(^2P\right) + N\left(^2P\right) \quad (7)$$

$$e + N_2 \rightarrow e + N_2\left(A_3\Sigma_u^+\right) \quad (8)$$

$$N\left(^2D\right) + O_2 \rightarrow NO + O\cdot \quad (9)$$

$$N\left(^2P\right) + O_2 \rightarrow NO + O\cdot \quad (10)$$

$$N_2\left(A_3\Sigma_u^+\right) + O_2 \rightarrow O\cdot + O\cdot + N_2 \quad (11)$$

$$e + O_2 \rightarrow e + O\cdot + O\cdot \quad (12)$$

$$O\cdot + O_2 + M \rightarrow O_3 + M \quad (13)$$

$$O_3 + NO \rightarrow NO_2 + O_2 \quad (14)$$

$$O\cdot + NO + M \rightarrow NO_2 + M \quad (15)$$

Figure 3c,d shows that the concentration of O_3 and NO_2 increased with the increase of SED. When the inlet 1-butene concentration was 100 ppm and SED increased from 33 to 203 J/L, the concentrations of O_3 and NO_2 increased from 514 to 1325 ppm and from 286 to 620 ppm, respectively. However, the increase of inlet 1-butene concentration led to an inhibition of the formation of O_3 and NO_2. For example, the O_3 concentration was reduced from 1021 to 533 ppm at an SED of 101 J/L as the inlet 1-butene concentration increased from 100 to 400 ppm. Meanwhile, the NO_2 concentration decreased from 520 to 367 ppm accordingly. The reason could be attributed to the consumption of energetic electrons and reactive species (e.g., N species and atomic O) during the process of 1-butene degradation [38]. In consideration of the significant formation of O_3 and NO_2 produced in the plasma process, many studies have reported that packing catalysts downstream of the DBD reactor could consume these byproducts effectively [39,40].

3.2. Effect of O_2/(N_2+O_2) Ratio

O_2 often plays an important role in VOC decomposition by affecting the electric field and the active species (Equations (9)–(15)). Three effects of O_2/(N_2+O_2) volume ratio on VOC decomposition performance based on the literature are shown below. First, the naphthalene decomposition efficiencies increased with the O_2/(N_2+O_2) volume ratio by the DBD plasma, indicating that the reactive species derived from O_2 mainly contributed to pollutant decomposition [41]. Next, the decomposition efficiencies of chlorodifluoromethane (CHF_2Cl) decreased with the increase of the O_2/(N_2+O_2) ratio because the reactive species from N_2 primarily contributed to the destruction of CHF_2Cl rather than those from O_2 [42]. Finally, the decomposition efficiencies of benzene and toluene reached a maximum value at 3–5% O_2 and then decreased with increasing O_2/(N_2+O_2) volume ratio. This result

might be caused by the fact that an enhanced generation of O atoms with the increase of O_2 concentration generally led to a higher degradation efficiency. However, with the further increase in O_2 concentration, more excited-state nitrogen species, O_3 and O atoms, were consumed through collisions between active particles (Equations (9)–(11), (14) and (15)), which would otherwise be used for destroying benzene [43,44]. In order to understand the influence of O_2 on the degradation of 1-butene, a series of experiments were conducted in which the O_2 volume ratio was varied from 0 to 20% at different SED, and the experimental results are illustrated in Figure 4. In this series of experiments, the inlet 1-butene concentration was maintained at around 200 ppm.

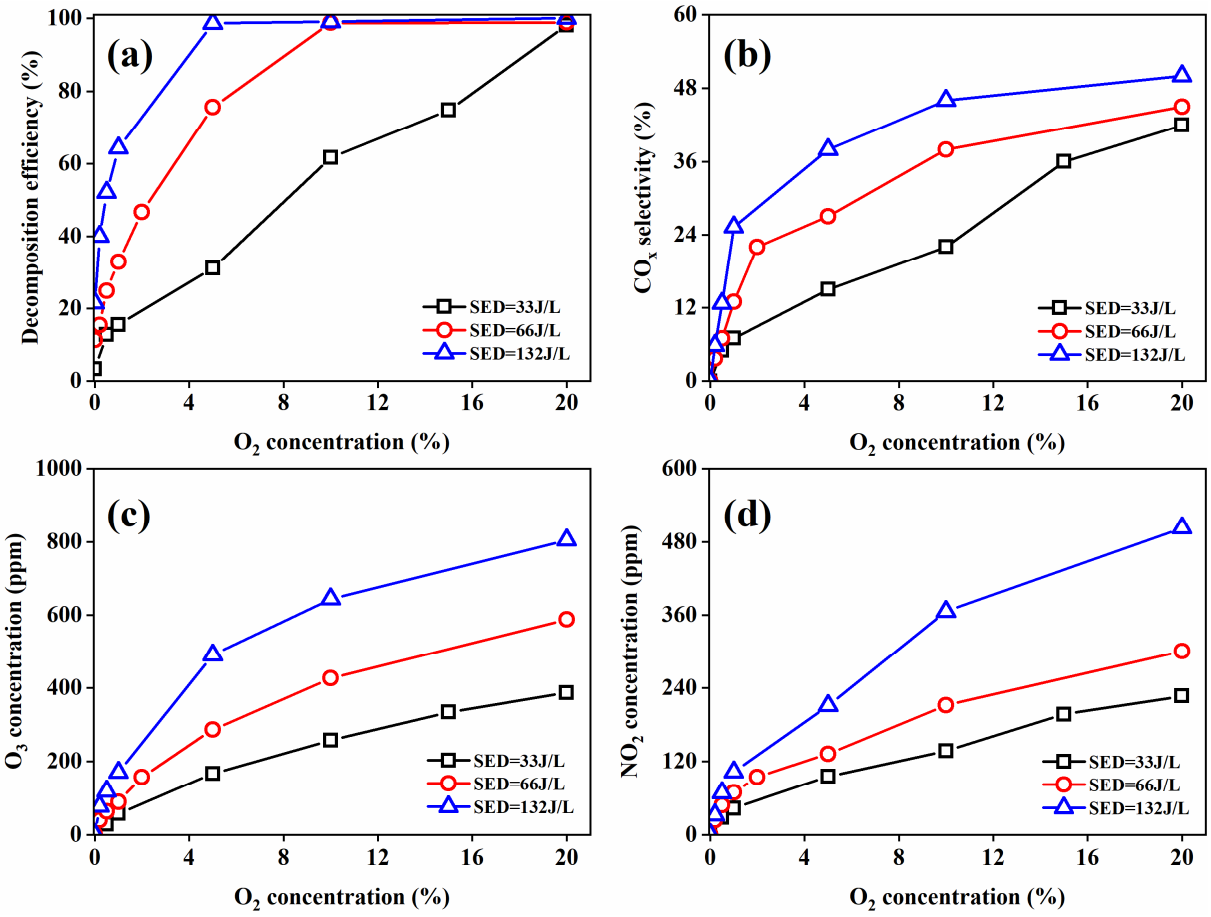

Figure 4. Effect of $O_2/(N_2+O_2)$ ratio on decomposition efficiency (**a**), CO_x selectivity (**b**), and the yield of O_3 (**c**) and NO_2 (**d**) (inlet 1-butene concentration 200 ppm).

As shown in Figure 4, the decomposition efficiency, CO_x selectivity, and the yield of O_3 and NO_2 increased rapidly with the O_2 concentration. Taking the SED of 66 J/L as an example, in the absence of O_2 in the gas, the 1-butene decomposition efficiency was only 11%, and CO_x, O_3 and NO_2 were not detected. When the O_2 volume ratio was raised to 20%, the 1-butene decomposition efficiency and CO_x selectivity increased to 99% and 45%, respectively, and the concentrations of O_3 and NO_2 were 588 ppm and 301 ppm, respectively. The increase of $O_2/(N_2+O_2)$ ratio in the gas was beneficial for 1-butene mineralization and oxidation product formation by facilitating the production of atomic O, which was concordant with the previous literature [41,43,44]. In addition, SED could enhance the decomposition efficiency and CO_x selectivity even at a low $O_2/(N_2+O_2)$ ratio. For example, when the $O_2/(N_2+O_2)$ volume ratio was 5% and SED was increased from 33 to 132 J/L, the decomposition efficiency increased from 31% to 99% and CO_x selectivity increased from 15% to 38%. The results suggest that raising the SED was one of the most effective ways to improve 1-butene degradation, especially at a low $O_2/(N_2+O_2)$ ratio.

3.3. Organic Byproduct Analysis

In order to illustrate the reaction mechanism of 1-butene destruction in N_2 and air, the gas compounds in the outlet of the TM-DBD reactor were analyzed by GC-MS at an SED of 51 and 203 J/L, respectively. The inlet concentration was maintained at around 300 ppm. The detected organic byproducts and their relative abundance under four different experimental conditions are presented in Figure 5 and Table 1. For 1-butene decomposition in N_2 plasma, hydrocarbon and oxy-organics were not found in the outlet gas even though the SED was increased. Moreover, CO_x has not been found either under similar experimental conditions, as shown in Figure 4b. These results indicate that the decomposition products of 1-butene mediated by the N reactive species may be in the main forms of nitrogenous organic compounds (such as amine, nitrile and nitrogen heterocyclic) [41]. Unfortunately, these nitrogenous organic compounds cannot be detected by GC-MS analysis. In comparison, abundant organic byproducts of 1-butene decomposition were found in air plasma, which included alcohol, aldehyde, ketone, acid and oxirane. With the SED raised from 51 to 203 J/L, the contents of formaldehyde, acetaldehyde, ethyl alcohol, acetic acid and propionic acid increased, while the contents of propionaldehyde, ethyl oxirane, butyraldehyde and formic acid decreased.

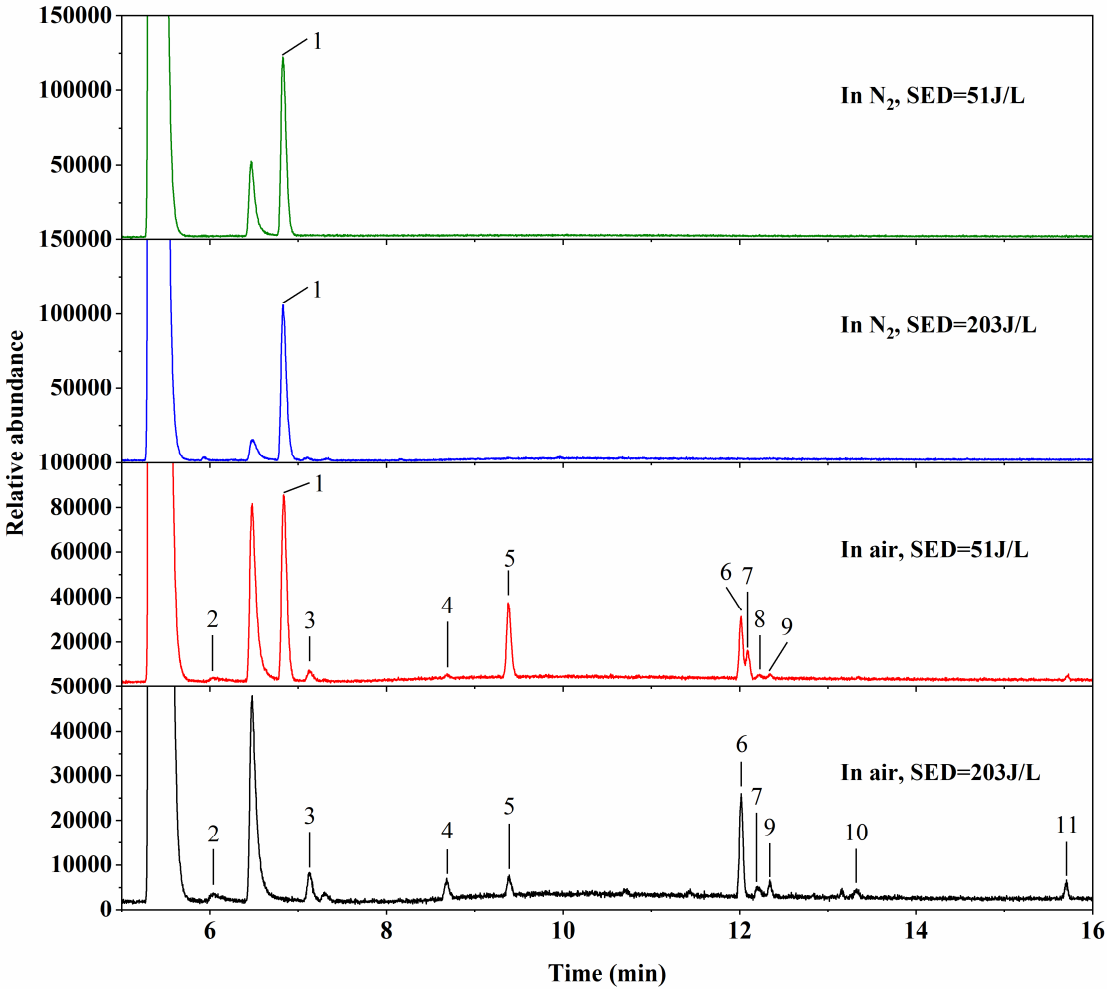

Figure 5. GC-MS spectra of organic byproducts in the outlet of TM-DBD under four experimental conditions.

Table 1. The organic byproducts detected in four experimental conditions.

Peak Numbers	Time (min)	Organic Compound	Structure	Relative Abundance			
				SED = 51 J/L in N_2	SED = 51 J/L in Air	SED = 203 J/L in N_2	SED = 203 J/L in Air
1	6.839	1-butene	$CH_2 = CHCH_2CH_3$	5,094,566	3,544,865	4,561,915	n.d
2	6.034	Formaldehyde	CH_2O	n.d	169,841	n.d	177,739
3	7.126	Acetaldehyde	CH_3CHO	n.d	215,131	n.d	263,062
4	8.686	Ethyl alcohol	CH_3CH_2OH	n.d	639,90	n.d	148,173
5	9.382	Propionaldehyde	CH_3CH_2CHO	n.d	1,231,359	n.d	147,682
6	12.017	Ethyl oxirane	$CH_3CH_2CH(O)CH_2$	n.d	840,904	n.d	704,603
7	12.091	Butyraldehyde	$CH_3CH_2CH_2CHO$	n.d	371,202	n.d	82,059
8	12.225	Formic acid	HCOOH	n.d	67,179	n.d	n.d
9	12.344	2-butanone	$CH_3COCH_2CH_3$	n.d	77,893	n.d	79,384
10	13.322	Acetic acid	CH_3COOH	n.d	n.d	n.d	63,755
11	15.705	Propionic acid	CH_3CH_2COOH	n.d	n.d	n.d	93,962

n.d: not detected.

3.4. Proposed Reaction Mechanism

Based on the intermediates detected by GC-MS analysis, three possible 1-butene decomposition pathways were proposed during the air plasma treatment. As shown in Figure 3, 200–1500 ppm O_3 were detected during the air plasma discharge procedure at a 1-butene concentration of 100–400 ppm. The cleavage of the double bonds of 1-butene (1) and related isomer 2-butene could easily take place by ozonolysis via 1,3-dipolar cycloaddition to give a carbonyl compound and a carbonyl oxide commonly called Criegee intermediates [45]. For Path A, due to the asymmetric structure of 1-butene (1), two zwitterion species, 5-O and 2-O, could be formed along with formaldehyde (2) and propanal (5), respectively. Criegee intermediates 5-O and 2-O could be trapped by nucleophiles, such as N-oxides, in air plasma. The generated species subsequently decomposed into related reduction products, propanal (5) and formaldehyde (2). With the aid of the active oxidants (i.e., $^{\bullet}OH$, $O^{\bullet}$), aldehyde compounds could proceed through further oxidation to produce the related acid propionic acid (11) and formic acid (8) [46], which could go through a direct decarbonylation process to furnish CO and H_2O. Additionally, after further oxidation of formic acid to carbonic acid (12), a decarboxylation reaction could take place to eliminate a carboxyl group and with the release of CO_2. As shown in Figure 3b, it suggests that CO and CO_2 originated in two independent ways, and it was easier to obtain CO than CO_2. It should be noted that other possible pathways from acid compounds to generate CO and CO_2 could not be completely excluded, especially in surroundings full of high-energy electrons. For Path B, in the discharge atmosphere, the charged 1-butene (1-H) was capable of isomerizing with the resonance structure charged 2-butene (1-H'). Owing to the symmetrical structure of 2-butene, only one zwitterion specie 3-O was obtained and then reduced to acetaldehyde (3). The acetaldehyde (3) could not only be sequentially reduced to alcohol (4) but also be oxidized to acetic acid (10). For Path C, 1-butene could also react with Criegee intermediates to generate the epoxidized compound (6). According to the breaking method of C-O bonds, routes a and b were proposed in Figure 6. The n-butylaldehyde (7) and 2-butanone (9) could be determined, accompanying the rupture of the correspondent C_2-O (route a) and C_1-O bonds (route b), respectively.

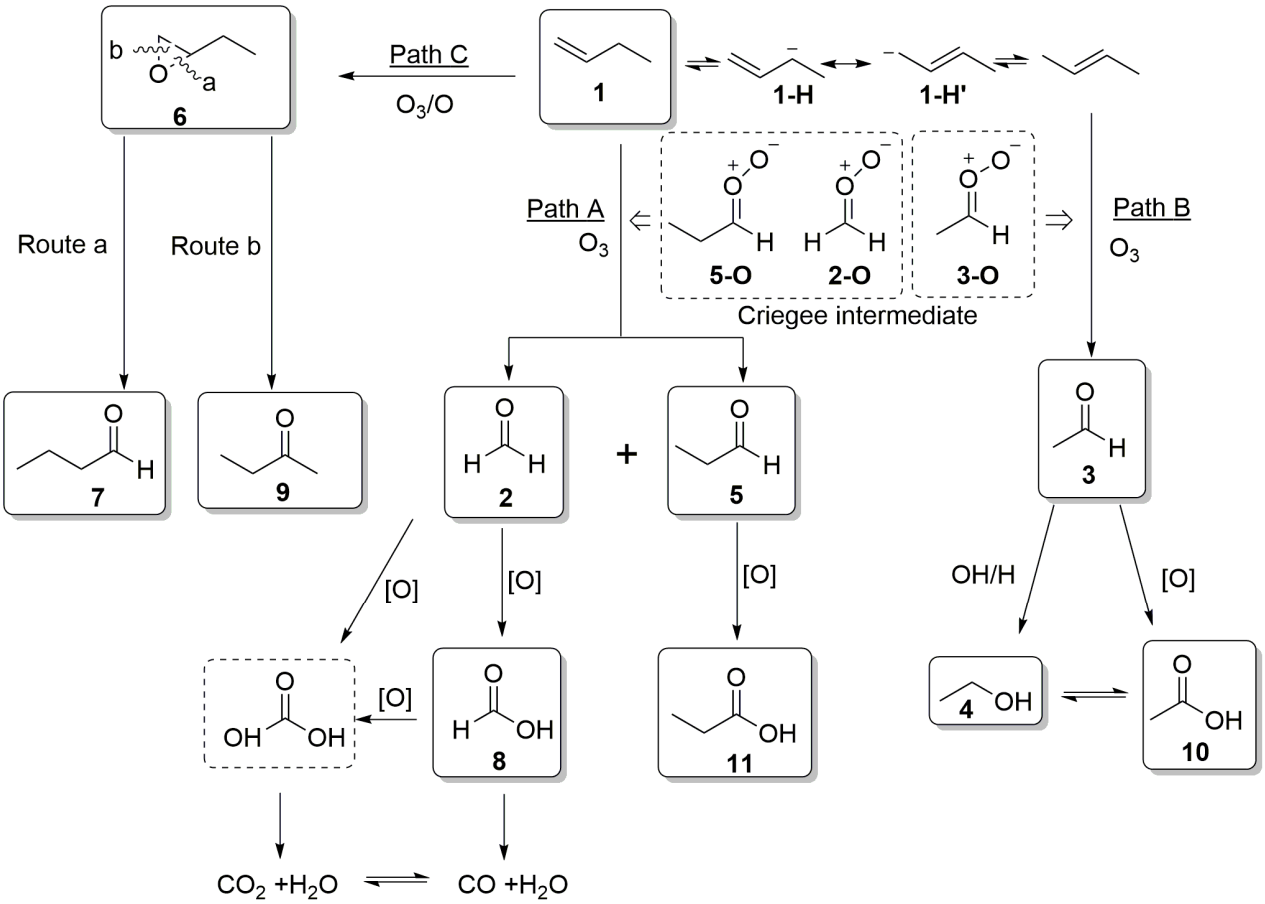

Figure 6. Proposed oxidation mechanism of 1-butene.

In addition, the amounts of the above organic byproducts were examined under conditions of 51 and 203 J/L, respectively. In Path A, as shown in Table 1, with the increase of SED, extra propionic acid (11) was found with the decrease of propionaldehyde (5), while formaldehyde (2) was enriched, and formic acid (8) totally vanished to form CO_x. (i.e., CO and CO_2). In detail, there was a slight increase in the amount of CO_2, while the amount of CO remained the same (Figure 3b). Active oxygen species were required for the formations of the CO_x precursors, i.e., formic acid and CO_2. The O_2 concentration plays a positive role in raising CO_x selectivity, which can be supported by the experimental results shown in Figure 4b. As for Path B, acetic acid (10) appeared along with both acetaldehyde (3) and ethyl alcohol (4). However, unlike Paths A and B, ethyl oxirane (6) and butyraldehyde (7) in Path C both declined, while 2-butanone (9) was well maintained. On the basis of the above results, ozonolysis of the olefins and the subsequent degradation reaction may be the dominant pathways rather than epoxidation.

4. Conclusions

In this study, we developed a TM-DBD reactor for the decomposition of 1-butene at ambient pressure, which is a typical gaseous pollutant in petrochemical exhaust gas. The results indicate that DBD plasma was an effective technology for removing a low 1-butene concentration of 100–400 ppm from the exhaust gas. First, the decomposition efficiency, CO_x selectivity and by-product yield were systematically studied with operating parameters (e.g., inlet concentration, SED). When SED reached 100 J/L, a decomposition efficiency of more than 99% and CO_x selectivity of at least 43% could be obtained; meanwhile, the production of O_3 and NO_2 were lower than 1021 ppm and 520 ppm, respectively. Second, the effect of $O_2/(N_2+O_2)$ ratio was also examined. The increasing $O_2/(N_2+O_2)$ ratio and SED were beneficial in improving the 1-butene decomposition and CO_x selectivity.

Finally, the degradation mechanism of 1-butene was proposed according to the analysis of organic byproducts. The main organic byproducts of 1-butene decomposition in air plasma consisted of alcohol, aldehyde, ketone and organic acid, as well as oxirane. Based on the above experimental results from the GC-MS analysis, three main pathways were proposed involving Criegee intermediates. In particular, ozonolysis of the olefins and the following reduction (Paths A and B) could be the dominant pathways rather than epoxidation (Path C), which was consistent with the GC-MS analysis results. In general, this study did not only offer an effective TM-DBD reactor for 1-butene decomposition but also illustrated the potential 1-butene degradation pathways, facilitating the industrial application of plasma technology for gaseous pollutant control. More importantly, these original data played a constructive role in promoting plasma industrialization, especially in the treatment of petrochemical waste gas.

Author Contributions: C.L.: conceptualization, methodology, investigation, data curation, formal analysis, writing original draft, writing—review and editing. X.Z.: investigation, formal analysis. S.W.: supervision, resources. Y.G. (Yafeng Guo): project administration, validation, writing—review & editing. Y.D.: formal analysis, methodology. Y.G. (Yinxia Guan): investigation. S.T.: formal analysis, validation, writing—review & editing. All authors have read and agreed to the published version of the manuscript.

Funding: This work was supported by the Science & Technology R&D Department of SINOPEC (no. KL323003, KL22059, and 321001).

Institutional Review Board Statement: Not applicable.

Informed Consent Statement: Not applicable.

Data Availability Statement: Not applicable.

Conflicts of Interest: The authors declare no conflict of interest.

References

1. Yang, Q.; Hou, R.; Sun, K. Tuning butene selectivities by cu modification on pd-based catalyst for the selective hydrogenation of 1,3-butadiene. *J. Catal.* **2019**, *374*, 12–23. [CrossRef]
2. Suprun, W.; Sadovskaya, E.M.; Rüdinger, C.; Eberle, H.J.; Lutecki, M.; Papp, H. Effect of water on oxidative scission of 1-butene to acetic acid over V_2O_5-TiO_2 catalyst. transient isotopic and kinetic study. *Appl. Catal. A* **2011**, *391*, 125–136. [CrossRef]
3. Masoori, M.; Nekoomanesh, M.; Posada-Pérez, S.; Rashedi, R.; Bahri-Laleh, N. A systematic study on the effect of co-catalysts composition on the performance of Ziegler-Natta catalyst in ethylene/1-butene co-polymerizations. *Polymer* **2022**, *261*, 125423. [CrossRef]
4. Zheng, W.; Zhao, Y.; Han, M.; Zhou, C.; He, A. Regulation of alkoxysilane on stereoregular polymerization of butene-1 catalyzed by $TiCl_4/MgCl_2$ ziegler-natta catalysts. *Polymer* **2021**, *228*, 123925. [CrossRef]
5. Zhao, R.; Wang, H.; Zhao, D.; Liu, R.; Liu, S.; Fu, J.; Zhang, Y.; Ding, H. Review on catalytic oxidation of VOCs at ambient temperature. *Int. J. Mol. Sci.* **2022**, *23*, 13739. [CrossRef] [PubMed]
6. Liu, Y.; Kong, L.; Liu, X.; Zhang, Y.; Zha, S. Characteristics, secondary transformation, and health risk assessment of ambient volatile organic compounds (VOCs) in urban beijing, china. *Atmos. Pollut. Res.* **2021**, *12*, 33–46. [CrossRef]
7. Yang, K.; Wang, C.; Xue, S.; Li, W.; Liu, J.; Li, L. The identification, health risks and olfactory effects assessment of VOCs released from the wastewater storage tank in a pesticide plant. *Ecotoxicol. Environ. Saf.* **2019**, *184*, 109665. [CrossRef]
8. Son, Y.S. Decomposition of VOCs and odorous compounds by radiolysis: A critical review. *Chem. Eng. J.* **2017**, *316*, 609–622. [CrossRef]
9. Mu, Y.; Williams, P.T. Recent advances in the abatement of volatile organic compounds (VOCs) and chlorinated-VOCs by non-thermal plasma technology: A review. *Chemosphere* **2022**, *308*, 136481. [CrossRef]
10. Veerapandian, S.; Leys, C.; Geyter, N.D.; Morent, R. Abatement of VOCs using packed bed non-thermal plasma reactors: A review. *Catalysts* **2017**, *7*, 113. [CrossRef]
11. Jiang, N.; Guo, L.; Qiu, C.; Zhang, Y.; Shang, K.; Lu, N.; Li, J.; Wu, Y. Reactive species distribution characteristics and toluene destruction in the three-electrode DBD reactor energized by different pulsed modes. *Chem. Eng. J.* **2018**, *350*, 12–19. [CrossRef]
12. Najafpoor, A.A.; Jafari, A.J.; Hosseinzadeh, A.; Jazani, R.K.; Bargozin, H. Optimization of non-thermal plasma efficiency in the simultaneous elimination of benzene, toluene, ethyl-benzene, and xylene from polluted airstreams using response surface methodology. *Environ. Sci. Pollut. Res.* **2018**, *25*, 233–241. [CrossRef] [PubMed]
13. Sharmin, S.; Arne, M.V.; Christophe, L.; Nathalie, D.G.; Rino, M. Abatement of VOCs with alternate adsorption and plasma-assisted regeneration: A review. *Catalysts* **2015**, *5*, 718–746.

14. Li, S.; Dang, X.; Yu, X.; Abbas, G.; Cao, L. The application of dielectric barrier discharge non-thermal plasma in VOCs abatement: A review. *Chem. Eng. J.* **2020**, *388*, 124275. [CrossRef]
15. Mustafa, M.F.; Fu, X.; Liu, Y.; Abbas, Y.; Wang, H.; Lu, W. Volatile organic compounds (VOCs) removal in non-thermal plasma double dielectric barrier discharge reactor. *J. Hazard. Mater.* **2018**, *347*, 317–324. [CrossRef]
16. Thomas, J.M.; Kaufman, F. Rate constants of the reactions of metastable $N_2(A^3\Sigma^+{}_u)$ in v=0, 1, 2, and 3 with ground state O_2 and O. *J. Chem. Phys.* **1985**, *83*, 2900–2903. [CrossRef]
17. Garscadden, A.; Nagpal, R. Non-equilibrium electronic and vibrational kinetics in H_2-N_2 and H_2 discharges. *Plasma Sources Sci. Technol.* **1995**, *4*, 268–280. [CrossRef]
18. Cernogora, G.; Hochard, L.; Touzeau, M.; Ferreira, C.M. Population of $N_2(A_3\Sigma_u{}^+)$ metastable states in a pure nitrogen glow discharge. *J. Phys. B At. Mol. Phys.* **1981**, *14*, 2977–2987. [CrossRef]
19. Mok, Y.S.; Chang, M.N.; Cho, M.H.; Nam, I.S. Decomposition of volatile organic compounds and nitric oxide by nonthermal plasma discharge processes. *IEEE Trans. Plasma Sci.* **2002**, *30*, 408–416.
20. Aerts, R.; Tu, X.; Bie, C.D.; Whitehead, J.C.; Bogaerts, A. An investigation into the dominant reactions for ethylene destruction in non-thermal atmospheric plasmas. *Plasma Process. Polym.* **2012**, *9*, 994–1000. [CrossRef]
21. Karatum, O.; Deshusses, M.A. A comparative study of dilute VOCs treatment in a non-thermal plasma reactor. *Chem. Eng. J.* **2016**, *294*, 308–315. [CrossRef]
22. Rodrigues, A.; Tatibouët, J.M.; Fourré, E. Operando drift spectroscopy characterization of intermediate species on catalysts surface in VOC removal from air by non-thermal plasma assisted catalysis. *Plasma Chem. Plasma Process.* **2016**, *36*, 901–915. [CrossRef]
23. Ma, T.; Zhao, Q.; Liu, J.; Zhong, F. Study of humidity effect on benzene decomposition by the dielectric barrier discharge nonthermal plasma reactor. *Plasma Sci. Technol.* **2016**, *18*, 686–692. [CrossRef]
24. Schiavon, M.; Scapinello, M.; Tosi, P.; Ragazzi, M.; Torretta, V.; Rada, E.C. Potential of non-thermal plasmas for helping the biodegradation of volatile organic compounds (VOCs) released by waste management plants. *J. Clean. Prod.* **2015**, *104*, 211–219. [CrossRef]
25. Li, X.; Guo, T.; Peng, Z.; Xu, L.; Dong, J.; Cheng, P.; Zhou, Z. Real-time monitoring and quantification of organic by-products and mechanism study of acetone decomposition in a dielectric barrier discharge reactor. *Environ. Sci. Pollut. Res.* **2019**, *26*, 6773–6781. [CrossRef] [PubMed]
26. Blin-Simiand, N.; Pasquiers, S.; Jorand, F.; Postel, C.; Vacher, J.R. Removal of formaldehyde in nitrogen and in dry air by a DBD: Importance of temperature and role of nitrogen metastable states. *J. Phys. D Appl. Phys.* **2009**, *42*, 122003. [CrossRef]
27. Trinh, Q.H.; Mok, Y.S. Effect of the adsorbent/catalyst preparation method and plasma reactor configuration on the removal of dilute ethylene from air stream. *Catal. Today* **2015**, *256*, 170–177. [CrossRef]
28. Trinh, Q.H.; Lee, S.B.; Mok, Y.S. Removal of ethylene from air stream by adsorption and plasma-catalytic oxidation using silver-based bimetallic catalysts supported on zeolite. *J. Hazard. Mater.* **2015**, *285*, 525–534. [CrossRef] [PubMed]
29. Gandhi, M.S.; Mok, Y.S. Catalytic non-thermal plasma decomposition of ethylene by using ZrO_2 nanoparticles. *Plasma Process. Polym.* **2015**, *12*, 214–224. [CrossRef]
30. Zhang, J.; Liu, J.; Zhang, R.; Hou, H.; Chen, S.; Zhang, Y. Destruction of gaseous styrene with a low-temperature plasma induced by a tubular multilayer dielectric barrier discharge. *Plasma Sci. Technol.* **2015**, *17*, 50–55. [CrossRef]
31. Manley, T.C. The electric characteristics of the ozonator discharge. *Trans. Electrochem. Soc.* **1943**, *84*, 83–96. [CrossRef]
32. Ma, Y.; Wang, X.; Ning, P.; Cheng, C.; Xu, K.; Wang, F.; Bian, Z.; Yan, S. Conversion of COS by corona plasma and the effect of simultaneous removal of COS and dust. *Chem. Eng. J.* **2016**, *290*, 328–334. [CrossRef]
33. Malik, M.A.; Kolb, J.F.; Sun, Y.H.; Schoenbach, K.H. Comparative study of NO removal in surface-plasma and volume-plasma reactors based on pulsed corona discharges. *J. Hazard. Mater.* **2011**, *197*, 220–228. [CrossRef] [PubMed]
34. Eliasson, B.; Hirth, M.; Kogelschatz, U. Ozone synthesis from oxygen in dielectric barrier discharges. *J. Phys. D Appl. Phys.* **1987**, *20*, 1421–1437. [CrossRef]
35. Herron, J.T. Evaluated chemical kinetics data for reactions of $N(^2D)$, $N(^2P)$, and $N_2(A_3\Sigma_u{}^+)$ in the gas phase. *J. Phys. Chem. Ref. Data* **1999**, *28*, 1453–1483. [CrossRef]
36. Böhmer, E.; Hack, W. Rate constants for the reactions of $N_2(A^3\Sigma_u{}^+, v')$ with $O_3(\tilde{X}_1A_1)$. *Phys. Chem.* **1991**, *95*, 1688–1690. [CrossRef]
37. Umemoto, H.; Hachiya, N.; Matsunaga, E.; Suda, A.; Kawasaki, M. Rate constants for the deactivation of $N(2^2D)$ by simple hydride and deuteride molecules. *Chem. Phys. Lett.* **1998**, *296*, 203–207. [CrossRef]
38. Vandenbroucke, A.M.; Morent, R.; Geyter, N.D.; Leys, C. Non-thermal plasmas for non-catalytic and catalytic VOC abatement. *J. Hazard. Mater.* **2011**, *195*, 30–54. [CrossRef] [PubMed]
39. Bo, Z.; Hao, H.; Yang, S.; Zhu, J.; Yan, J.; Cen, K. Vertically-oriented graphenes supported Mn_3O_4 as advanced catalysts in post plasma-catalysis for toluene decomposition. *Appl. Surf. Sci.* **2018**, *436*, 570–578. [CrossRef]
40. Chang, T.; Shen, Z.; Huang, Y.; Lu, J.; Ren, D.; Sun, J.; Cao, J.; Liu, H. Post-plasma-catalytic removal of toluene using MnO_2-Co_3O_4 catalysts and their synergistic mechanism. *Chem. Eng. J.* **2018**, *348*, 15–25. [CrossRef]
41. Wu, Z.; Wang, J.; Han, J.; Yao, S.; Xu, S.; Martin, P. Naphthalene decomposition by dielectric barrier discharges at atmospheric pressure. *IEEE Trans. Plasma Sci.* **2016**, *45*, 154–161. [CrossRef]
42. Mok, Y.S.; Lee, S.B.; Chang, M.S. Destruction of chlorodifluoromethane (CHF_2Cl) by using dielectric barrier discharge plasma. *IEEE Trans. Plasma Sci.* **2009**, *37*, 449–455.

43. Jiang, N.; Lu, N.; Shang, K.; Li, J.; Wu, Y. Innovative approach for benzene degradation using hybrid surface/packed-bed discharge plasmas. *Environ. Sci. Technol.* **2013**, *47*, 9898–9903. [CrossRef] [PubMed]
44. Kim, H.H.; Ogata, A.; Futamura, S. Oxygen partial pressure-dependent behavior of various catalysts for the total oxidation of VOCs using cycled system of adsorption and oxygen plasma. *Appl. Catal. B* **2008**, *79*, 356–367. [CrossRef]
45. Hassan, Z.; Stahlberger, M.; Rosenbaum, N.; Bräse, S. Criegee intermediates beyond ozonolysis: Synthetic and mechanistic insights. *Angew. Chem. Int. Ed. Engl.* **2021**, *60*, 15138–15152. [CrossRef]
46. Jalan, A.; Allen, J.W.; Green, W.H. Chemically activated formation of organic acids in reactions of the Criegee intermediate with aldehydes and ketones. *Phys. Chem. Chem. Phys.* **2013**, *15*, 16841–16852. [CrossRef]